GhostSR: Learning Ghost Features for Efficient Image Super-Resolution

Ying Nie[1], Kai Han[1], Zhenhua Liu[1,3], An Xiao[1], Yiping Deng[2], Chunjing Xu[1],Yunhe Wang[1]

[1] Noah's Ark Lab, Huawei Technologies

[2] Central Software Institution, Huawei Technologies   [3] Peking University

{ying.nie, kai.han, an.xiao, yiping.deng, xuchunjing, yunhe.wang}@huawei.com

liu-zh@pku.edu.cn

Abstract

Modern single image super-resolution (SISR) system based on convolutional neural networks (CNNs) achieves fancy performance while requires huge computational costs. The problem on feature redundancy is well studied in visual recognition task, but rarely discussed in SISR. Based on the observation that many features in SISR models are also similar to each other, we propose to use shift operation to generate the redundant features (i.e. Ghost features). Compared with depth-wise convolution which is not friendly to GPUs or NPUs, shift operation can bring practical inference acceleration for CNNs on common hardware. We analyze the benefits of shift operation for SISR and make the shift orientation learnable based on Gumbel-Softmax trick. For a given pre-trained model, we first cluster all filters in each convolutional layer to identify the intrinsic ones for generating intrinsic features. Ghost features will be derived by moving these intrinsic features along a specific orientation. The complete output features are constructed by concatenating the intrinsic and ghost features together. Extensive experiments on several benchmark models and datasets demonstrate that both the non-compact and lightweight SISR models embedded in our proposed module can achieve comparable performance to that of their baselines with large reduction of parameters, FLOPs and GPU latency. For instance, we reduce the parameters by 47%, FLOPs by 46% and GPU latency by 41% of EDSR $\times 2$ network without significant performance degradation.

1. Introduction

Single image super-resolution (SISR) is a classical low-level computer vision task, which aims at recovering a high-resolution (HR) image from its corresponding low-resolution (LR) image. Since multiple HR images could be downsampled to the same LR image, SISR is an ill-posed reverse problem. Recently, deep convolutional neural network (CNN) based methods have made significant improve-
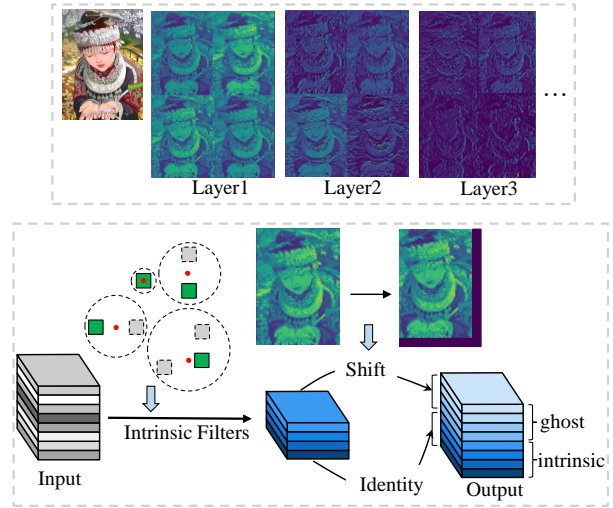

Figure 1. Visualization of features generated by different layers in VDSR [23], which obviously has many similar features (Top). The redundant features (*i.e.* ghost features) can be generated by cheap operation such as shift based on intrinsic features. The intrinsic features are generated by intrinsic filters, which are selected via clustering pre-trained model (Bottom).

ment on SISR through carefully designed network architectures. The pioneer work SRCNN [8] which contains only three convolutional layers outperforms the previous non-deep learning methods. Subsequently, the capacity of CNNs is further excavated with deeper and more complex architectures [23, 28, 52, 53], and significantly improved the SISR results. However, compared with image classification networks, the remarkable performance of super-resolution networks usually involve more number of floating-point operations (FLOPs). For example, the FLOPs for processing a single 224×224 image using $\times 2$ EDSR [28] and ResNet-50 [16] are 2270.9G and 4.1G, respectively. Therefore, compression and acceleration for super-resolution networks is more urgent and practical.

Recently, several works on compression and acceleration for super-resolution networks have been proposed. Namhyuk *et al.* developed CARN [1] which addressed ef-

ficient SISR by combining the efficient residual block with group convolution. Zheng *et al.* introduced IDN [21] which applied knowledge distillation for enhancing the performance of lightweight SISR models. ESRN [38] utilized neural architecture search technique for searching efficient SISR models. PAN [54] constructed a pretty concise and effective network with pixel attention scheme. The basic operations in those works are still conventional convolution, which do not consider the redundancy in features and the practical speed in common hardwares.

Feature redundancy widely exists in deep convolutional neural networks [15, 27]. Since most of the existing SISR models need to preserve the overall texture and color information of the input images, there are inevitably many similar features in each layer as observed in the top of Figure 1. To reduce the overall FLOPs and maintain the performance of heavy CNN architectures, the redundant features *i.e.* ghost features can be generated using cheaper operations based on the intrinsic features as discussed in GhostNet [12]. GhostNet is a backbone designed for image recognition task which involves massive depth-wise convolution for generating the ghost features with lower computational cost. Although depth-wise convolution theoretically has large compression ratio over regular convolution, its practical speed on common hardwares with large computing power such as GPU and NPU is very disappointing [33]. For instance, given a 256×256 input image on single GPU V100 platform, the latency of regular convolution with 64 output channels is 0.15ms, but the latency of the combined module of 32-channel regular convolution and 32-channel depth-wise convolution is increased to 0.19ms. Considering that the size of images captured by modern intelligent terminals are mostly in 4K format, the efficiency of SISR models should be maintained on the common platforms with large computing power.

In this paper, we introduce the efficient GhostSR method for SISR to alleviate the massive computations caused by convolution. We propose to first identify the intrinsic filters via clustering a pre-trained model, and the features generated by the intrinsic filters are taken as intrinsic features. Then, a GPU-efficient shift operation is explored in which the orientation for each layer is trained using the Gumbel-Softmax trick. We then thoroughly analyze its functionality by embedding it into the existing SISR models. Specifically, the shift operation moves the intrinsic features along a specific orientation to get ghost features. The complete output features are then constructed by concatenating the intrinsic and the ghost features. The shift operation can emphasize more edge and texture information which can be seen as a compensation to the conventional convolution filters. Moreover, with our efficient CUDA implementation of shift operation, we bring a practical acceleration on mainstream GPUs. The effectiveness of the proposed method is carefully verified on several SISR benchmark models and datasets. In particular, by exploiting the proposed method, We can obtain comparable performance and visual quality to that of their baseline models with large reduction of parameters, FLOPs and GPU latency.

The rest of the paper is organized as follows: Section 2 briefly introduces the related work in model compression and efficient super-resolution fields. We introduce our method for developing GhostSR networks in Section 3. Experiments and corresponding analysis are described in Section 4. Section 5 concludes the paper.

2. Related Works

In this section, we revisit the existing model compression methods on general vision tasks and image super-resolution task.

2.1. Model Compression

In order to compress deep CNNs, a series of methods have been proposed which include network pruning [14, 27, 7, 3, 41], knowledge distillation [18, 34, 47, 4] and low-bit quantization [6, 56, 36, 49]. Han *et al.* [14] removed the connections whose weights are lower than a certain threshold in network. Ding *et al.* [7] proposed Centripetal SGD to gradually approach filters in the same cluster and eventually the same for network slimming. Hinton *et al.* [18] introduced knowledge distillation to improve the performance of student model by inheriting knowledge from a teacher model. Courbariaux *et al.* [6] quantized the weights and activations into 1-bit value to maximize the compression and acceleration of the network. In addition, lightweight network architecture design has demonstrated its advantages in constructing more efficient neural network architectures [19, 51, 45, 48, 1, 13]. MobileNets [19, 35] are a series of lightweight networks based on depthwise convolution. TinyNet [13] introduced a new model shrinking method that scales network depth, width and resolution simultaneously. Wu *et al.* [46] first proposed the shift operation which moves the input features horizontally or vertically, then Jeon *et al.* [22] and chen *et al.* [5] further made the shift operation learnable in visual recognition task. Recently, Han *et al.* [12] analyzed the redundancy in features and introduced a novel GhostNet to generate more features with fewer parameters.

2.2. Efficient Image Super-Resolution

Numerous milestone works based on deep neural network have been proposed in image super-resolution task [8, 23, 40, 28, 53, 52, 37]. However, these works are difficult to deploy on resource-limited devices due to their heavy computation cost and memory footprint. To this end, efficient model design for super-resolution is attracting widespread attention. FSRCNN [9] firstly accelerated

the SR network by a compact hourglass-shape architecture. DRCN [24]and DRRN [39] adopted recursive layers to build deep network with fewer parameters. CARN [1] reduced the calculation of SR networks by combining the efficient residual block with group convolution. Attention mechanism is also introduced to find the most informative region to reconstruct high-resolution image with better quality [54, 32, 30, 52]. To improve the performance of lightweight networks, distillation has been excavated to transfer the knowledge from big teacher networks to tiny student network [21, 10]. Recently, neural architecture search has also been employed to exploit the efficient architecture for image super-resolution [38, 11, 26].

3. Approach

In this section, we describe the details of our GhostSR method for efficient image super-resolution.

3.1. Shift for Generating Ghost Features

The CNN-based super-resolution models consist of massive convolution computations. For a vanilla convolutional layer, producing the output features $Y \in \mathbb{R}^{c_o \times h \times w}$ requires $c_o \cdot h \cdot w \cdot c_i \cdot s \cdot s$ FLOPs where c_o, h, w, c_i, $s \times s$ are the number of output channels, the height of output, the width of output, the number of input channels and the kernel size. The computational cost of convolution consumes much energy and inference time. On the other hand, we observe that some features in SR network is similar to another ones, $i.e.$, these redundant features can be viewed as ghosts of the other intrinsic features, as shown in the top of Figure 1. In fact, redundant features can provide more texture and high-frequency information in addition to the intrinsic features, which cannot be directly removed as discussed in GhostNet [12]. Instead of discarding, we propose to utilize a more efficient operator, $i.e.$ shift operation, to generate them.

Supposing the ratio of ghost features is λ, we have $(1 - \lambda)c_o$ intrinsic features and λc_o ghost features. We use regular convolution to produce the intrinsic features $I \in \mathbb{R}^{(1-\lambda)c_o \times h \times w}$. For the ghost features $G \in \mathbb{R}^{\lambda c_o \times h \times w}$, we generate them through shift operation based on I since shift is cheap yet has many advantages, $i.e.$, more texture information and larger receptive field, which will be discussed in detail later. Formally, the vertical and horizontal offsets to be shifted are $i_o - d - 1$ and $j_o - d - 1$, where $1 \leq i_o \leq 2d + 1$, $1 \leq j_o \leq 2d + 1$, and d is the maximum offset, then the element in position (y, x) of G can be obtained as:

$$G_{y,x,c_1} = \sum_{i=0}^{2d+1} \sum_{j=0}^{2d+1} I_{y+i-d-1,x+j-d-1,c_2} W_{i,j} \quad (1)$$

where c_1 and c_2 are the channel index of ghost features and the corresponding index of intrinsic features. All the elements in $W \in \{0,1\}^{(2d+1) \times (2d+1)}$ are 0 except that the value in the offset position is 1:

$$W_{i,j} = \begin{cases} 1, & \text{if } i = i_o \text{ and } j = j_o, \\ 0, & \text{otherwise.} \end{cases} \quad (2)$$
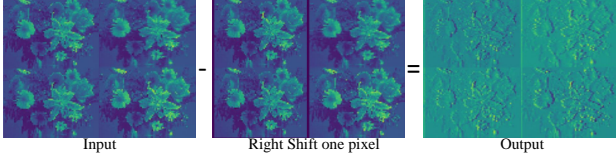
Finally, we concatenate the intrinsic and ghost features together as the complete output: $Y = [I, G]$. Compared to original convolution layer, our method cuts the FLOPs directly by a ratio of λ since shift operation is FLOPs-free. More importantly, with our efficient CUDA implementation of shift operation, we bring a practical inference acceleration on GPU-like devices.

Benefits of shift for image super-resolution. Super-resolution aims at recovering a high-resolution image from its corresponding low-resolution image. The enhanced high frequency information such as texture could be helpful for improving the quality of recovered high-resolution image [52, 55]. Given a input feature map F_I, we shift F_I one pixel to the right across all channels, and pad the vacant position with zeros to get the shifted feature maps $F_{I'}$. The texture information can be generated by $F_{I'} - F_I$, as shown in the top of Figure 2. In convolution neural network, the vanilla features and the shifted features are concatenated together to be processed by next layer's convolution operation. The convolution operation can be seen as a more complex operation involving subtraction, which can enhance the high frequency information to some extent.
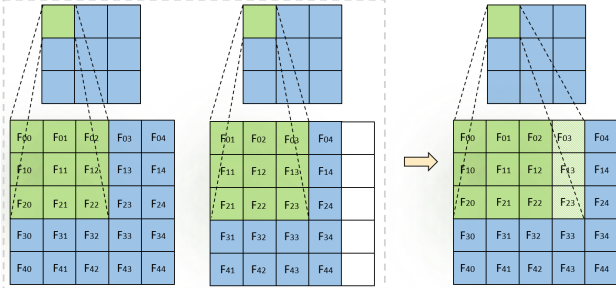
In addition, the combination of two spatially dislocated feature maps can enlarge the receptive field of CNNs, which is critical for super-resolution task [43, 17]. In other words, the shift operation of feature maps provides a spatial information communication of convolution filters. For instance, when shift a feature map one pixel to the left, the receptive field of the same location on the next layer's feature map shift one pixel to the left correspondingly. The convolution operation performed on the combination of dislocation feature maps results in a wider receptive field, which is demonstrated in the bottom of Figure 2.

Last but not least, as opposed to depth-wise convolution's fragmented memory footprints, shift operation is more efficient in terms of practical speed, which will be compared in detail in the experiments section.

Learnable shift. The shift operation in Eq. 1 can be viewed as a special case of depth-wise convolution where only one weight is 1 and the others are 0. In order to flexibly adjust the offset of intrinsic features during training process, we propose to make the offset weight W learnable. However, the one-hot values in W make it difficult to optimize the weights. We utilize Gumbel-Softmax trick to address this issue. The Gumbel-Softmax trick feed-forwards the

(a) Enhance high frequency information.

(b) Enlarge receptive field

Figure 2. Benefits of shifting the intermediate layer features for image super-resolution task.

one-hot signal and back-propagates the soft signal, which solves the non-derivableness of sampling from categorical distribution.

We create a proxy soft weight $W' \in \mathbb{R}^{(2d+1)\times(2d+1)}$ for representing the inherent values of one-hot W. A noise $N \in \mathbb{R}^{(2d+1)\times(2d+1)}$ is randomly sampled from the exponentially decayed Gumbel distribution:

$$N_{i,j} = -\log(-\log(U_{i,j})) * a^{t-1}, \qquad (3)$$

where $U_{ij} \sim U(0,1)$, a is the hyper-parameter of exponential distribution and t is current training epoch. The one-hot weight W is relaxed as

$$S(W'_{i,j}) = \frac{e^{(W'_{i,j}+N_{i,j})/\tau}}{\sum_{i=0}^{2d+1}\sum_{j=0}^{2d+1} e^{(W'_{i,j}+N_{i,j})/\tau}}, \qquad (4)$$

where τ is the temperature to control the sharpness of the softmax function, and the function approximates the discrete categorical sampling. Then, we can obtain the values of offset indices as

$$i_o, j_o = \arg\max_{i,j} S(W'). \qquad (5)$$

During feed-forward process, the values of W can be computed as Eq. 2. As for the back-propagation process, we use a straight-through estimator, that is, the derivative $\frac{\partial W}{\partial W'}$ is approximated calculated using the derivative of Eq. 4:

$$\frac{\partial W}{\partial W'} = \frac{\partial S(W')}{\partial W'}. \qquad (6)$$

Then, we can optimize the shift weight W and the other weights in neural network end-to-end. After training, we pick the position of the maximum value as the shift offset position and construct the inference graph of GhostSR networks.

3.2. Ghost Features in Pre-Trained Model

We aim to generate the redundant features in a more efficient operation. In particular, we first generate $(1-\lambda)c_o$ features as intrinsic features, then use shift operation to generate the other features as ghost features based on the intrinsic features, and finally concatenate the intrinsic and ghost features together as the complete output features. If we train a GhostSR model from scratch, the indices c_1 and c_2 in Eq. 1 are set simply by order. If a pre-trained vanilla SR model is provided, we can utilize the relation of intrinsic and ghost features for better performance.

For a pre-trained SR model, we aim to replace the convolutional filters generating redundant features with shift operation. However, for a certain layer in network, it is not clear which part of the output features are intrinsic and which should be ghost features. We address this issue by clustering filters in the pre-trained model layer by layer, and the features generated by the filter which is closet to the cluster centroid are taken as intrinsic features. In particular, we use clustering method *e.g.* k-means, to generate cluster groups with high inter-cluster distance and low intra-cluster distance. We vectorize the weights of all the convolutional filters from $[c_o, c_i, s, s]$ to $[c_o, c_i \times s \times s]$ and obtain vectors $\{f_1, f_2, \cdots, f_{c_o}\}$. We aim to divide all the weight kernels into $(1-\lambda)c_o$ clusters $\mathcal{G} = \{G_1, G_2, ..., G_{(1-\lambda)c_o}\}$. Any pair of points in one cluster should be as close to each other as possible:

$$\min_{\mathcal{G}} \sum_{k=1}^{(1-\lambda)c_o} \sum_{i \in G_k} ||f_i - \mu_k||_2^2 \qquad (7)$$

where μ_k is the mean of points in cluster G_k. We use k-means algorithm for clustering filters with the objective function as in Eq. 7. In each cluster, the cluster centroid can be viewed as the intrinsic filter, and the features generated by the intrinsic filters as intrinsic features. For cluster clusters with only one filter, we take the only filter as intrinsic filter. For cluster clusters with multiple filters, the centroid may not really exist in the original weight kernels, so we select the filter which is nearest to the centroid as intrinsic filter, and the index of intrinsic filters can be formulated as

$$\mathbb{I}_k = \begin{cases} i \in G_k, & \text{if } |G_k| = 1, \\ \arg\min_{i \in G_k} ||f_i - \mu_k||_2^2, & \text{otherwise.} \end{cases} \qquad (8)$$

The set of intrinsic indices is $\mathbb{I} = \{\mathbb{I}_1, \mathbb{I}_2, \cdots, \mathbb{I}_{(1-\lambda)c_o}\}$ whose corresponding filters are preserved as intrinsic filters, and the other ghost filters are replaced by shift operations. When clustering the next layer connected to the previous layer, to maintain the consistency of the clustering channels across the adjacent layers, we use the previous layer's intrinsic indices to screen out the useful input channels of the
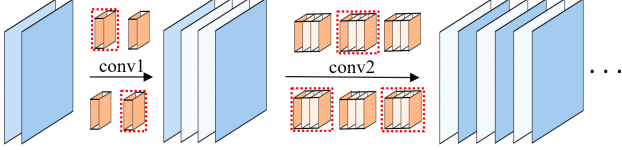
Figure 3. An illustration of our clustering procedure, the red dotted boxes indicate the intrinsic filters.

filters F' in the next layer as illustrated in Figure 3. Formally,

$$F' \leftarrow F'[:, \mathbb{I}, :, :], \qquad (9)$$

After finding the intrinsic filters in each layers of the pre-trained model, we assign the corresponding weight in pre-trained model to the intrinsic filters. Thus, we can maximally utilize the information in pre-trained model to identify intrinsic features and inheriting pre-trained filters for better performance. Finally, our approach is summarized in Alg. 1.

Algorithm 1 Learning Ghost Features for Efficient SISR.

Input: Paired training data; Pre-trained regular convolution models; The selected layers to be compressed.
Output: A well-trained lightweight GhostSR network.
 1: Cluster the first convolutional layer that needs to be compressed (Eq. 7), then select the intrinsic filter in each cluster (Eq. 8).
 2: Calculate the features of other layers for clustering (Eq. 9, 7), and select intrinsic filters (Eq. 8).
 3: Assign the corresponding weight in pre-trained model to the intrinsic filters W^I.
 4: **repeat**
 5:     Output the intrinsic features I convolved by W^I;
 6:     Calculate the transformed proxy soft weights $S(W')$ of shift operation by softmax function (Eq. 3, 4);
 7:     Calculate the one-hot weights W of shift operation based on $S(W')$ (Eq. 5, 2);
 8:     Output the ghost features G convolved by $detach(W\text{-}S(W'))\text{+}S(W')$ based on I;
 9:     Feed-forward the concatenated features: $Y = [I, G]$;
10:     Calculate the gradients of W^I and W' by standard back-propagation, and update W^I and W' simultaneously via Adam.
11: **until** convergence

---

4. Experiments

In this section, we conduct extensive experiments on non-compact and lightweight networks. The detailed quantitative and qualitative evaluations are provided to verify the effectiveness of our method. Thorough ablation study and analysis are also provided to further investigate the proposed scheme. We conduct experiments on NVIDIA Tesla V100 GPU and implement our method in PyTorch framework.

4.1. Experimental Settings

Datasets and Metrics. To evaluate the performance of our method, following the setting of [28, 53, 1], we use 800 images from DIV2K [42] dataset to train our models. In order to compare with other state-of-the-art methods, we report our result on four standard benchmark datasets: Set5 [2], Set14 [50], B100 [31] and Urban100 [20]. The LR images are generated by bicubic down-sampling and the SR results are evaluated by PSNR and SSIM [44] on Y channel of YCbCr space.

Training Details. We use four famous SR models as our baselines: EDSR [28], RDN [53], CARN [1] and CARN_M [1]. These models have various numbers of parameters ranging from 0.41M to 43.71M (million). To improve the performance of the models embedded in our method, we do not replace the regular convolution in the first and the last layers in these networks, and the point-wise convolution is also kept unchanged if encountered in the middle layers. In all our experiments, the ratio of ghost features is set to 0.5, the hyper-parameter a in Eq. 3 and the temperature τ in Eq. 4 are set to 0.97 and 1, respectively.

During training, we crop 16 images with 48×48 patch size from the LR images on every GPU for training. The input examples are augmented by random horizontal flipping and 90° rotating. In addition, all the images are pre-processed by subtracting the mean RGB value of the DIV2K dataset. To optimize the model, we use ADAM optimizer [25] with $\beta_1 = 0.9$, $\beta_2 = 0.999$, and $\epsilon = 10^{-8}$. We train EDSR and RDN for 300 epochs by single-scale training scheme, and train CARN and CARN_M for 1200 epochs by multi-scale training scheme. The initial learning rate is set to 1e-4 for all models and reduced by cosine learning rate decay method [29].

4.2. Comparisons with Baselines

Quantitative Evaluation. In Table 1, we report the quantitative results of the baseline convolutional networks and our Ghost versions for scaling factor ×2, ×3 and ×4. The results of Conv type are obtained by our re-training, which are similar to the results in the original papers. In addition, the FLOPs and latency are calculated through a $3 \times 512 \times 512$ image and on single NVIDIA V100 GPU.

For the non-compact EDSR and RDN, when the regular convolution is replaced with the shift operation, the parameters and FLOPs are reduced by nearly half without significant performance degradation. Moreover, with our efficient CUDA implementation of shift operation, GhostSR brings a practical acceleration on GPUs. For instance, GhostSR

Table 1. Quantitative results of baseline convolutional networks and their Ghost versions for scaling factor ×2, ×3 and ×4. FLOPs and latency are calculated through a $3 \times 512 \times 512$ image and on single NVIDIA V100 GPU. The results of Conv type are obtained by our re-training.

Scale	Model	Type	Params (M)	FLOPs (G)	Latency (ms)	Set5 PSNR/SSIM	Set14 PSNR/SSIM	B100 PSNR/SSIM	Urban100 PSNR/SSIM
×2	EDSR	Conv	40.72	10679	943	38.22 / 0.9612	33.86 / 0.9201	32.34 / 0.9018	32.92 / 0.9356
		GhostSR	21.63	5734	557	↓0.07 / ↓0.0002	↓0.00 / ↓0.0008	↓0.05 / ↓0.0006	↓0.27 / ↓0.0023
	RDN	Conv	22.11	5798	672	38.25 / 0.9614	33.97 / 0.9205	32.34 / 0.9017	32.90 / 0.9355
		GhostSR	11.54	3011	465	↓0.06 / ↓0.0003	↓0.04 / ↑0.0001	↓0.02 / ↓0.0003	↓0.11 / ↓0.0012
	CARN	Conv	1.59	317	49	37.88 / 0.9601	33.54 / 0.9173	32.14 / 0.8990	31.96 / 0.9267
		GhostSR	1.19	219	40	↓0.00 / ↓0.0000	↓0.00 / ↑0.0002	↓0.03 / ↓0.0003	↓0.09 / ↓0.0009
	CARN_M	Conv	0.41	114	49	37.72 / 0.9595	33.31 / 0.9150	31.97 / 0.8970	31.25 / 0.9194
		GhostSR	0.33	105	46	↑0.02 / ↑0.0001	↓0.00 / ↑0.0003	↑0.01 / ↑0.0003	↑0.08 / ↑0.0008
×3	EDSR	Conv	43.71	11462	1024	34.67 / 0.9293	30.56 / 0.8466	29.26 / 0.8094	28.78 / 0.8649
		GhostSR	24.53	6516	645	↓0.08 / ↓0.0008	↓0.12 / ↓0.0021	↓0.07 / ↓0.0017	↓0.28 / ↓0.0053
	RDN	Conv	22.33	5849	677	34.69 / 0.9296	30.54 / 0.8467	29.26 / 0.8093	28.79 / 0.8654
		GhostSR	11.73	3062	472	↓0.09 / ↓0.0011	↓0.04 / ↓0.0008	↓0.04 / ↓0.0009	↓0.20 / ↓0.0041
	CARN	Conv	1.59	373	58	34.35 / 0.9266	30.32 / 0.8415	29.08 / 0.8043	28.05 / 0.8499
		GhostSR	1.19	276	49	↓0.08 / ↓0.0004	↓0.02 / ↓0.0005	↓0.01 / ↓0.0004	↓0.08 / ↓0.0019
	CARN_M	Conv	0.41	130	55	34.04 / 0.9242	30.06 / 0.8364	28.91 / 0.8001	27.46 / 0.8363
		GhostSR	0.33	121	53	↑0.01 / ↑0.0001	↑0.03 / ↑0.0006	↑0.02 / ↑0.0007	↑0.08 / ↑0.0021
×4	EDSR	Conv	43.14	13175	1198	32.46 / 0.8984	28.81 / 0.7874	27.73 / 0.7416	26.60 / 0.8019
		GhostSR	23.93	8229	819	↓0.14 / ↓0.0013	↓0.08 / ↓0.0021	↓0.07 / ↓0.0022	↓0.28 / ↓0.0078
	RDN	Conv	22.21	5958	702	32.49 / 0.8987	28.83 / 0.7875	27.72 / 0.7416	26.59 / 0.8023
		GhostSR	11.64	3171	485	↓0.15 / ↓0.0016	↓0.11 / ↓0.0024	↓0.06 / ↓0.0021	↓0.24 / ↓0.0074
	CARN	Conv	1.59	493	76	32.16 / 0.8943	28.59 / 0.7810	27.58 / 0.7355	26.03 / 0.7830
		GhostSR	1.19	395	68	↓0.05 / ↓0.0007	↓0.02 / ↓0.0008	↓0.02 / ↓0.0007	↓0.05 / ↓0.0020
	CARN_M	Conv	0.41	162	68	31.79 / 0.8890	28.35 / 0.7747	27.40 / 0.7292	25.51 / 0.7652
		GhostSR	0.33	150	66	↑0.06 / ↑0.0014	↑0.05 / ↑0.0015	↑0.03 / ↑0.0014	↑0.08 / ↑0.0032

reduces the parameters by 47%, FLOPs by 46% and latency by 41% of EDSR ×2 network with no significant performance degradation. For the lightweight CARN and CARN_M, the parameters, FLOPs and GPU latency are also reduced by different sizes. For example, the number of group-convolution in CARN_M is only six, when we replace the group-convolution in CARN_M with our GhostSR module, the GPU latency decreases less than other models. However, the performance of GhostSR CARN_M even all slightly outperforms regular convolution on four standard benchmark datasets, we attribute it to the superiority of shift operation and the excavation of information in pre-trained models.

Qualitative Evaluation. The qualitative evaluations on various datasets are shown in Figure 4. We choose the most challenging ×4 task to reveal the difference of visual quality between the regular convolution version and our ghost version. For both the non-compact networks and the lightweight networks, with our method, the details and textures generated by shift operation are basically the same as those by regular convolution.

4.3. Comparisons under FLOPs Budget

In table 2, we report the quantitative results of different methods of reducing FLOPs for CARN. Conv-0.88× means to directly reduce the number of channels in each layer of the network to 0.88 times the original channel. Conv-Prune indicates that the state-of-the-art pruning method in [7] is used to reduce the number of network channels. We reimplement the centripetal SGD in [7] into centripetal Adam and use it to train the image super-resolution task. In addition, we also compare the results of replacing the shift operation in our method with depth-wise convolution, which denoted by Ghost-DW. CARN itself is a lightweight network, and directly reducing the width of each layer of the network will bring a greater performance drop. For instance, compared with the original CARN (denoted as Conv-1×),
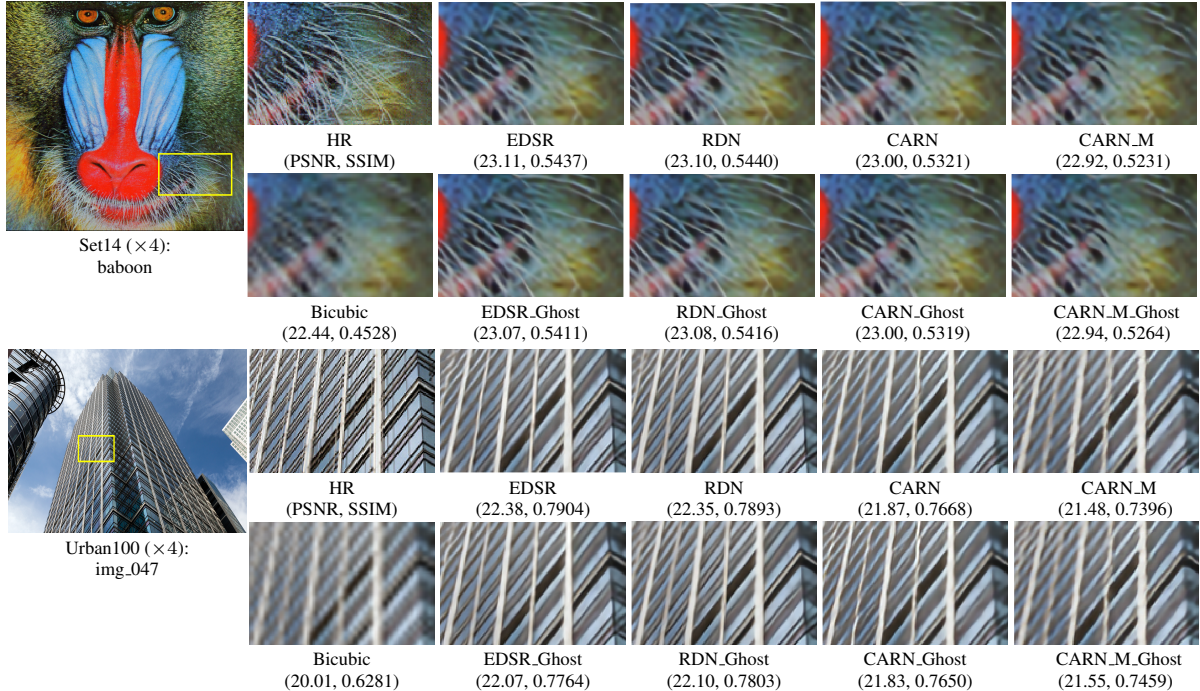
Figure 4. Visual comparisons for ×4 images on Set14 and Urban100 datasets. For all the shown examples, with our method, the details and textures generated by shift operation are approximately the same as those by regular convolution.
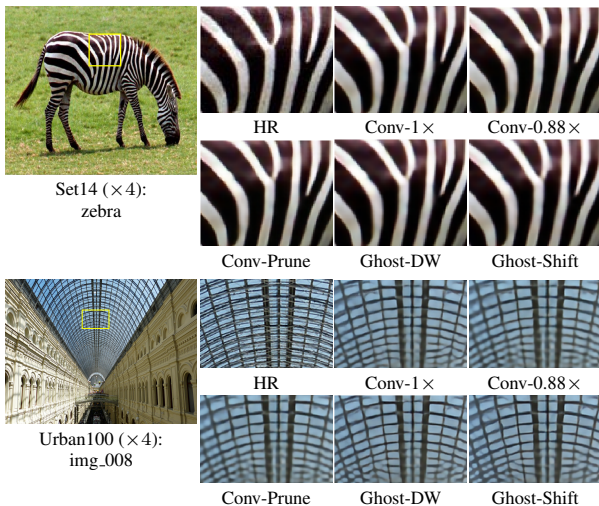

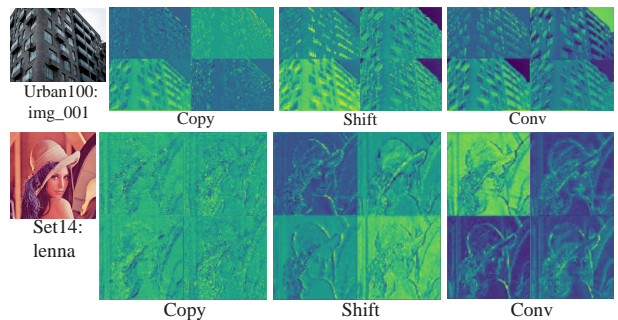Figure 5. Visual comparisons of ×4 images by different CARN.

Figure 6. Visualization of features generated at the same layer by different CARN. The learnable shift operation extracts more textures than simple copying.

the PSNR of Conv-0.88× and Conv-Prune are reduced by 0.15db and 0.12db for ×2 scale on Urban100 dataset, respectively. When the shift operation in our GhostSR module is replaced with depth-wise convolution, the performance of CARN is slightly improved, but the latency is greatly increased. For example, the PSNR of ×4 Ghost-DW exceeds Ghost-Shift by 0.04db on Urban100 dataset, however, the latency is correspondingly increased from 68ms to 76ms.

Figure 5 visualizes the ×4 images generated by different type of CARN. The visual quality of the images generated by reducing the number of network channels is obviously

degraded, and our method produces the images of quality close to the original network. We attribute it to the characteristics of shift operation, which can partially compensate for the performance degradation caused by the reduction in channels. For example, the left side of the enlarged area of img_008 generated by Conv-0.88× is blurred compared to our method.

4.4. Ablation Study

In this section, we conduct a series of comparison experiments to validate the effectiveness of the proposed schemes in our method, the ×4 results are reported in Table 3. For the option that does not use the learnable shift scheme, we replace the shift operation with a simple copy operation, and for the option that does not use the information in pre-

Table 2. Comparisons of different CARN under similar FLOPs budget, the FLOPs and latency are calculated through a $3 \times 512 \times 512$ image and on single NVIDIA V100 GPU.

Scale	Type	Params (M)	FLOPs (G)	Latency (ms)	Set5 PSNR/SSIM	Set14 PSNR/SSIM	B100 PSNR/SSIM	Urban100 PSNR/SSIM
×2	Conv-1×	1.59	317	49	37.88 / 0.9601	33.54 / 0.9173	32.14 / 0.8990	31.96 / 0.9267
	Conv-0.88×	1.22	243	42	↓0.01 / ↓0.0000	↓0.05 / ↓0.0004	↓0.04 / ↓0.0004	↓0.15 / ↓0.0016
	Conv-Prune [7]	1.22	243	42	↓0.00 / ↓0.0000	↓0.03 / ↓0.0002	↓0.04 / ↓0.0003	↓0.12 / ↓0.0013
	Ghost-DW [12]	1.26	221	47	↓0.00 / ↓0.0000	↓0.00 / ↑0.0001	↓0.02 / ↓0.0001	↓0.05 / ↓0.0006
	Ghost-Shift (ours)	1.19	219	40	↓0.00 / ↓0.0000	↓0.00 / ↑0.0002	↓0.03 / ↓0.0003	↓0.09 / ↓0.0010
×3	Conv-1×	1.59	373	58	34.35 / 0.9266	30.32 / 0.8415	29.08 / 0.8043	28.05 / 0.8499
	Conv-0.88×	1.22	286	50	↓0.12 / ↓0.0009	↓0.08 / ↓0.0014	↓0.07 / ↓0.0014	↓0.16 / ↓0.0031
	Conv-Prune [7]	1.22	286	50	↓0.11 / ↓0.0007	↓0.07 / ↓0.0009	↓0.05 / ↓0.0010	↓0.13 / ↓0.0026
	Ghost-DW [12]	1.26	278	56	↓0.05 / ↓0.0002	↓0.04 / ↓0.0005	↓0.02 / ↓0.0006	↓0.05 / ↓0.0008
	Ghost-Shift (ours)	1.19	276	49	↓0.08 / ↓0.0004	↓0.02 / ↓0.0005	↓0.01 / ↓0.0004	↓0.08 / ↓0.0019
×4	Conv-1×	1.59	493	76	32.16 / 0.8943	28.59 / 0.7810	27.58 / 0.7355	26.03 / 0.7830
	Conv-0.88×	1.22	383	66	↓0.10 / ↓0.0011	↓0.08 / ↓0.0015	↓0.06 / ↓0.0018	↓0.13 / ↓0.0043
	Conv-Prune [7]	1.22	383	66	↓0.08 / ↓0.0007	↓0.07 / ↓0.0012	↓0.02 / ↓0.0005	↓0.10 / ↓0.0031
	Ghost-DW [12]	1.26	398	76	↓0.02 / ↓0.0005	↓0.00 / ↓0.0003	↓0.01 / ↓0.0005	↓0.01 / ↓0.0008
	Ghost-Shift (ours)	1.19	395	68	↓0.05 / ↓0.0007	↓0.02 / ↓0.0008	↓0.02 / ↓0.0007	↓0.05 / ↓0.0020

Table 3. Ablation study of the proposed method for ×4 CARN.

Model	Architecture		Set5 PSNR/SSIM	Set14 PSNR/SSIM	B100 PSNR/SSIM	Urban100 PSNR/SSIM
	Learnable Shift	Pre-trained Model				
GhostSR CARN 1	×	×	31.91/0.8925	28.39/0.7779	27.47/0.7328	25.79/0.7765
GhostSR CARN 2	×	✓	32.07/0.8933	28.53/0.7798	27.53/0.7339	25.93/0.7794
GhostSR CARN 3	✓	×	32.05/0.8929	28.51/0.7793	27.52/0.7337	25.90/0.7786
GhostSR CARN 4	✓	✓	32.11/0.8936	28.57/0.7802	27.56/0.7348	25.98/0.7810
Original CARN	–	–	32.16/0.8943	28.59/0.7810	27.58/0.7355	26.03/0.7830

trained models, we train the SISR network from scratch. When neither learnable shift scheme nor the information in pre-trained models is used, the PSNR of GhostSR is 0.24db lower than that of conventional CARN on Urban100 dataset. When only the information in pre-trained models or the learnable shift scheme is used, the PSNR drops by 0.1db and 0.13db on Urban100 dataset, respectively. When both of them are used, the PSNR degradation relative to conventional CARN is reduced to 0.05db.

Figure 6 visualizes the features generated at the same layer for three versions of CARN: simple copy operation, learnable shift operation and regular convolution operation. The simple copy version and the learnable shift version of CARN are both trained based on the pre-trained model using the aforementioned clustering procedure. The features of img_001 and lenna are generated in the first and third residual-block of CARN, respectively. From Figure 6, the learnable shift operation extracts textures similar to that of the regular convolution, and more than the simple copy operation.

5. Conclusion

This paper proposes the GhostSR method for efficient single image super-resolution models. We first study the feature redundancy in convolutional layers and introduce a novel learnable shift operation to replace a large proportion of conventional filters for generating ghost features. Then, we present a procedure of clustering pre-trained models to select the intrinsic filters for generating intrinsic features. Thus, we can effectively learn and identify the intrinsic features and ghost features simultaneously. Compared to depth-wise convolution, shift operation can bring a practical inference acceleration on GPUs. We empirically analyze the benefits of using shift operation for SISR task. Extensive experiments on several benchmark models and datasets demonstrate that both the non-compact and lightweight SISR models embedded in our GhostSR method can achieve comparable quantitative result and qualitative quality to that of their baselines with large practical inference acceleration.

References

[1] Namhyuk Ahn, Byungkon Kang, and Kyung-Ah Sohn. Fast, accurate, and lightweight super-resolution with cascading residual network. In *Proceedings of the European Conference on Computer Vision (ECCV)*, pages 252–268, 2018. 1, 2, 3, 5

[2] Marco Bevilacqua, Aline Roumy, Christine Guillemot, and Marie Line Alberi-Morel. Low-complexity single-image super-resolution based on nonnegative neighbor embedding. 2012. 5

[3] Hanting Chen, Yunhe Wang, Han Shu, Yehui Tang, Chunjing Xu, Boxin Shi, Chao Xu, Qi Tian, and Chang Xu. Frequency domain compact 3d convolutional neural networks. In *CVPR*, 2020. 2

[4] Hanting Chen, Yunhe Wang, Han Shu, Changyuan Wen, Chunjing Xu, Boxin Shi, Chao Xu, and Chang Xu. Distilling portable generative adversarial networks for image translation. In *AAAI*, 2020. 2

[5] Weijie Chen, Di Xie, Yuan Zhang, and Shiliang Pu. All you need is a few shifts: Designing efficient convolutional neural networks for image classification. In *Proceedings of the IEEE Conference on Computer Vision and Pattern Recognition*, pages 7241–7250, 2019. 2

[6] Matthieu Courbariaux, Yoshua Bengio, and Jean-Pierre David. Binaryconnect: Training deep neural networks with binary weights during propagations. In *NeurIPS*, pages 3123–3131, 2015. 2

[7] Xiaohan Ding, Guiguang Ding, Yuchen Guo, and Jungong Han. Centripetal sgd for pruning very deep convolutional networks with complicated structure. In *Proceedings of the IEEE Conference on Computer Vision and Pattern Recognition*, pages 4943–4953, 2019. 2, 6, 8

[8] Chao Dong, Chen Change Loy, Kaiming He, and Xiaoou Tang. Learning a deep convolutional network for image super-resolution. In *European conference on computer vision*, pages 184–199. Springer, 2014. 1, 2

[9] Chao Dong, Chen Change Loy, and Xiaoou Tang. Accelerating the super-resolution convolutional neural network. In *European conference on computer vision*, pages 391–407. Springer, 2016. 2

[10] Qinquan Gao, Yan Zhao, Gen Li, and Tong Tong. Image super-resolution using knowledge distillation. In *Asian Conference on Computer Vision*, pages 527–541. Springer, 2018. 3

[11] Yong Guo, Yongsheng Luo, Zhenhao He, Jin Huang, and Jian Chen. Hierarchical neural architecture search for single image super-resolution. *arXiv preprint arXiv:2003.04619*, 2020. 3

[12] Kai Han, Yunhe Wang, Qi Tian, Jianyuan Guo, Chunjing Xu, and Chang Xu. Ghostnet: More features from cheap operations. In *Proceedings of the IEEE/CVF Conference on Computer Vision and Pattern Recognition*, pages 1580–1589, 2020. 2, 3, 8

[13] Kai Han, Yunhe Wang, Qiulin Zhang, Wei Zhang, Chunjing Xu, and Tong Zhang. Model rubik's cube: Twisting resolution, depth and width for tinynets. *NeurIPS*, 2020. 2

[14] Song Han, Huizi Mao, and William J Dally. Deep compression: Compressing deep neural networks with pruning, trained quantization and huffman coding. *arXiv preprint arXiv:1510.00149*, 2015. 2

[15] Song Han, Huizi Mao, and William J Dally. Deep compression: Compressing deep neural networks with pruning, trained quantization and huffman coding. In *ICLR*, 2016. 2

[16] Kaiming He, Xiangyu Zhang, Shaoqing Ren, and Jian Sun. Deep residual learning for image recognition. In *CVPR*, pages 770–778, 2016. 1

[17] Zewei He, Yanpeng Cao, Lei Du, Baobei Xu, Jiangxin Yang, Yanlong Cao, Siliang Tang, and Yueting Zhuang. Mrfn: Multi-receptive-field network for fast and accurate single image super-resolution. *IEEE Transactions on Multimedia*, 22(4):1042–1054, 2019. 3

[18] Geoffrey Hinton, Oriol Vinyals, and Jeff Dean. Distilling the knowledge in a neural network. *arXiv preprint arXiv:1503.02531*, 2015. 2

[19] Andrew G Howard, Menglong Zhu, Bo Chen, Dmitry Kalenichenko, Weijun Wang, Tobias Weyand, Marco Andreetto, and Hartwig Adam. Mobilenets: Efficient convolutional neural networks for mobile vision applications. *arXiv preprint arXiv:1704.04861*, 2017. 2

[20] Jia-Bin Huang, Abhishek Singh, and Narendra Ahuja. Single image super-resolution from transformed self-exemplars. In *Proceedings of the IEEE conference on computer vision and pattern recognition*, pages 5197–5206, 2015. 5

[21] Zheng Hui, Xiumei Wang, and Xinbo Gao. Fast and accurate single image super-resolution via information distillation network. In *CVPR*, pages 723–731, 2018. 2, 3

[22] Yunho Jeon and Junmo Kim. Constructing fast network through deconstruction of convolution. In *Advances in Neural Information Processing Systems*, pages 5951–5961, 2018. 2

[23] Jiwon Kim, Jung Kwon Lee, and Kyoung Mu Lee. Accurate image super-resolution using very deep convolutional networks. In *Proceedings of the IEEE conference on computer vision and pattern recognition*, pages 1646–1654, 2016. 1, 2

[24] Jiwon Kim, Jung Kwon Lee, and Kyoung Mu Lee. Deeply-recursive convolutional network for image super-resolution. In *Proceedings of the IEEE conference on computer vision and pattern recognition*, pages 1637–1645, 2016. 3

[25] Diederik P Kingma and Jimmy Ba. Adam: A method for stochastic optimization. *arXiv preprint arXiv:1412.6980*, 2014. 5

[26] Royson Lee, Łukasz Dudziak, Mohamed Abdelfattah, Stylianos I Venieris, Hyeji Kim, Hongkai Wen, and Nicholas D Lane. Journey towards tiny perceptual super-resolution. *arXiv preprint arXiv:2007.04356*, 2020. 3

[27] Hao Li, Asim Kadav, Igor Durdanovic, Hanan Samet, and Hans Peter Graf. Pruning filters for efficient convnets. In *ICLR*, 2017. 2

[28] Bee Lim, Sanghyun Son, Heewon Kim, Seungjun Nah, and Kyoung Mu Lee. Enhanced deep residual networks for single image super-resolution. In *Proceedings of the IEEE conference on computer vision and pattern recognition workshops*, pages 136–144, 2017. 1, 2, 5

[29] Ilya Loshchilov and Frank Hutter. Sgdr: Stochastic gradient descent with warm restarts. *arXiv preprint arXiv:1608.03983*, 2016. 5

[30] Xiaotong Luo, Yuan Xie, Yulun Zhang, Yanyun Qu, Cuihua Li, and Yun Fu. Latticenet: Towards lightweight image super-resolution with lattice block. 3

[31] David Martin, Charless Fowlkes, Doron Tal, and Jitendra Malik. A database of human segmented natural images and its application to evaluating segmentation algorithms and measuring ecological statistics. In *Proceedings Eighth IEEE International Conference on Computer Vision. ICCV 2001*, volume 2, pages 416–423. IEEE, 2001. 5

[32] Abdul Muqeet, Jiwon Hwang, Subin Yang, Jung Heum Kang, Yongwoo Kim, and Sung-Ho Bae. Ultra lightweight image super-resolution with multi-attention layers. *arXiv preprint arXiv:2008.12912*, 2020. 3

[33] Ilija Radosavovic, Raj Prateek Kosaraju, Ross Girshick, Kaiming He, and Piotr Dollár. Designing network design spaces. In *CVPR*, 2020. 2

[34] Adriana Romero, Nicolas Ballas, Samira Ebrahimi Kahou, Antoine Chassang, Carlo Gatta, and Yoshua Bengio. Fitnets: Hints for thin deep nets. In *ICLR*, 2015. 2

[35] Mark Sandler, Andrew Howard, Menglong Zhu, Andrey Zhmoginov, and Liang-Chieh Chen. Mobilenetv2: Inverted residuals and linear bottlenecks. In *Proceedings of the IEEE conference on computer vision and pattern recognition*, pages 4510–4520, 2018. 2

[36] Mingzhu Shen, Kai Han, Chunjing Xu, and Yunhe Wang. Searching for accurate binary neural architectures. In *ICCV Workshops*, 2019. 2

[37] Dehua Song, Yunhe Wang, Hanting Chen, Chang Xu, Chunjing Xu, and DaCheng Tao. Addersr: Towards energy efficient image super-resolution. *arXiv preprint arXiv:2009.08891*, 2020. 2

[38] Dehua Song, Chang Xu, Xu Jia, Yiyi Chen, Chunjing Xu, and Yunhe Wang. Efficient residual dense block search for image super-resolution. In *AAAI*, pages 12007–12014, 2020. 2, 3

[39] Ying Tai, Jian Yang, and Xiaoming Liu. Image super-resolution via deep recursive residual network. In *Proceedings of the IEEE conference on computer vision and pattern recognition*, pages 3147–3155, 2017. 3

[40] Ying Tai, Jian Yang, Xiaoming Liu, and Chunyan Xu. Memnet: A persistent memory network for image restoration. In *Proceedings of the IEEE international conference on computer vision*, pages 4539–4547, 2017. 2

[41] Yehui Tang, Yunhe Wang, Yixing Xu, Dacheng Tao, Chunjing Xu, Chao Xu, and Chang Xu. Scop: Scientific control for reliable neural network pruning. In *NeurIPS*, 2020. 2

[42] Radu Timofte, Eirikur Agustsson, Luc Van Gool, Ming-Hsuan Yang, and Lei Zhang. Ntire 2017 challenge on single image super-resolution: Methods and results. In *Proceedings of the IEEE conference on computer vision and pattern recognition workshops*, pages 114–125, 2017. 5

[43] Ruxin Wang, Mingming Gong, and Dacheng Tao. Receptive field size versus model depth for single image super-resolution. *IEEE Transactions on Image Processing*, 29:1669–1682, 2019. 3

[44] Zhou Wang, Alan C Bovik, Hamid R Sheikh, and Eero P Simoncelli. Image quality assessment: from error visibility to structural similarity. *IEEE transactions on image processing*, 13(4):600–612, 2004. 5

[45] Bichen Wu, Xiaoliang Dai, Peizhao Zhang, Yanghan Wang, Fei Sun, Yiming Wu, Yuandong Tian, Peter Vajda, Yangqing Jia, and Kurt Keutzer. Fbnet: Hardware-aware efficient convnet design via differentiable neural architecture search. In *Proceedings of the IEEE Conference on Computer Vision and Pattern Recognition*, pages 10734–10742, 2019. 2

[46] Bichen Wu, Alvin Wan, Xiangyu Yue, Peter Jin, Sicheng Zhao, Noah Golmant, Amir Gholaminejad, Joseph Gonzalez, and Kurt Keutzer. Shift: A zero flop, zero parameter alternative to spatial convolutions. In *Proceedings of the IEEE Conference on Computer Vision and Pattern Recognition*, pages 9127–9135, 2018. 2

[47] Yixing Xu, Yunhe Wang, Hanting Chen, Kai Han, XU Chunjing, Dacheng Tao, and Chang Xu. Positive-unlabeled compression on the cloud. In *NeurIPS*, 2019. 2

[48] Zhaohui Yang, Yunhe Wang, Xinghao Chen, Boxin Shi, Chao Xu, Chunjing Xu, Qi Tian, and Chang Xu. Cars: Continuous evolution for efficient neural architecture search. In *CVPR*, 2020. 2

[49] Zhaohui Yang, Yunhe Wang, Kai Han, Chunjing Xu, Chao Xu, Dacheng Tao, and Chang Xu. Searching for low-bit weights in quantized neural networks. In *NeurIPS*, 2020. 2

[50] Roman Zeyde, Michael Elad, and Matan Protter. On single image scale-up using sparse-representations. In *International conference on curves and surfaces*, pages 711–730. Springer, 2010. 5

[51] Xiangyu Zhang, Xinyu Zhou, Mengxiao Lin, and Jian Sun. Shufflenet: An extremely efficient convolutional neural network for mobile devices. In *Proceedings of the IEEE conference on computer vision and pattern recognition*, pages 6848–6856, 2018. 2

[52] Yulun Zhang, Kunpeng Li, Kai Li, Lichen Wang, Bineng Zhong, and Yun Fu. Image super-resolution using very deep residual channel attention networks. In *Proceedings of the European Conference on Computer Vision (ECCV)*, pages 286–301, 2018. 1, 2, 3

[53] Yulun Zhang, Yapeng Tian, Yu Kong, Bineng Zhong, and Yun Fu. Residual dense network for image super-resolution. In *Proceedings of the IEEE conference on computer vision and pattern recognition*, pages 2472–2481, 2018. 1, 2, 5

[54] Hengyuan Zhao, Xiangtao Kong, Jingwen He, Yu Qiao, and Chao Dong. Efficient image super-resolution using pixel attention. *arXiv preprint arXiv:2010.01073*, 2020. 2, 3

[55] Fuqiang Zhou, Xiaojie Li, and Zuoxin Li. High-frequency details enhancing densenet for super-resolution. *Neurocomputing*, 290:34–42, 2018. 3

[56] Shuchang Zhou, Yuxin Wu, Zekun Ni, Xinyu Zhou, He Wen, and Yuheng Zou. Dorefa-net: Training low bitwidth convolutional neural networks with low bitwidth gradients. *arXiv preprint arXiv:1606.06160*, 2016. 2